SAIC-94/1151:APPAT-166
October 19, 1994

STRUCTURE AND DYNAMICS OF THE SOLAR CORONA

Science Applications International Corporation
An Employee-Owned Company

FINAL REPORT

1993-1994

ON

CONTRACT NASW-4579

D. D. SCHNACK, PRINCIPAL INVESTIGATOR

10260 Campus Point Drive, San Diego, California 92121 (619) 546-6000

Other SAIC Offices: Albuquerque, Boston, Colorado Springs, Dayton, Huntsville, Las Vegas, Los Angeles, McLean, Oak Ridge, Orlando, Palo Alto, Seattle, and Tucson

TABLE OF CONTENTS

LIST OF FIGURES

STRUCTURE AND DYNAMICS OF THE SOLAR CORONA

1. INTRODUCTION

In this document, Science Application International Corp. (SAIC) reports the results of a three-year study of the heating and large scale dynamics of the solar corona. We have used advanced computational techniques to study dynamics related to coronal heating and coronal mass ejections. In particular, we have:

1. Used a three-dimensional, time-dependent, resistive MHD code to study the dynamical response of a model corona to continuous, slow, random magnetic footpoint displacements in the photosphere. A statistical steady-state model corona was obtained in which the input Poynting flux was balanced by Ohmic dissipation. The resulting corona was characterized by filamentary current structures. A high Reynolds' number parameter regime was identified in which dynamical, transient reconnection events occurred.

2. Performed model three-dimensional numerical simulations of the response of the corona to simple smooth braiding flows in the photosphere to illustrate and understand the spontaneous formation of current filaments. Magnetic reconnection was also observed in these calculations.

3. Obtained two-dimensional, steady-state helmet streamer configurations by determining the time asymptotic state of the interaction of an initially one-dimensional transonic solar wind with a spherical potential dipole field. These calculations were performed in axially symmetric spherical geometry including gravity, density and pressure variations, and self-consistent characteristic boundary conditions. The resulting steady configuration had a two-dimensional, transonic solar wind, a partially open magnetic field, a sheet-like current structure, and flow stagnation under the helmet.

4. Studied the disruption of the steady-state helmet streamer configuration as a response to shearing of the magnetic footpoints of the closed field lines under the helmet. The disruption and magnetic reconnection produced a disconnected plasmoid that was ejected into the interplanetary medium. This event had several characteristics in common with coronal mass ejections (CMEs). In the same calculation we were able to follow the trajectory of the ejected plasmoid to the orbit of the earth (1 AU), and were able to determine the effect of the passage of this disturbance on the interplanetary magnetic field (IMF). The perturbation to the IMF was consistent with the onset of magnetic storms in the earth's magnetosphere.

A summary of these results is given in the following sections. Scientific papers reporting this work are in preparation.

2. MATHEMATICAL MODEL AND NUMERICAL SOLUTION

The appropriate physical model for low frequency, long wavelength motions of an electrically conducting fluid such as the solar corona is resistive magnetohydrodynamics. In cgs units, the equations of the model are

$$\frac{1}{c}\frac{\partial \mathbf{A}}{\partial t} = -\mathbf{E} \tag{1}$$

$$\mathbf{B} = \nabla \times \mathbf{A} \tag{2}$$

$$\mathbf{J} = \frac{c}{4\pi}\nabla \times \mathbf{B} \tag{3}$$

$$\mathbf{E} = -\frac{1}{c}\mathbf{v} \times \mathbf{B} + \eta \mathbf{J} \tag{4}$$

$$\rho\left(\frac{\partial \mathbf{v}}{\partial t} + \mathbf{v}\cdot\nabla\mathbf{v}\right) = -\nabla p + \frac{1}{c}\mathbf{J}\times\mathbf{B} + \rho\mathbf{g} + \rho\nu\nabla^2\mathbf{v} \tag{5}$$

$$\frac{\partial \rho}{\partial t} + \nabla\cdot\rho\mathbf{v} = 0 \tag{6}$$

$$\frac{\partial p}{\partial t} = -\nabla\cdot p\mathbf{v} - (\gamma-1)\, p\nabla\cdot\mathbf{v} + (\gamma-1)\eta\mathbf{J}^2 \tag{7}$$

where **A** is the vector potential, **B** is the magnetic flux density, **J** is the current density, **E** is the electric field, **v** is the fluid velocity, ρ is the mass density, p is the pressure, **g** is the gravitational acceleration, γ is the ratio of specific heats, c is the speed of light, η is the electrical resistivity, and ν is an artificial viscosity.

Equations (1–7) are solved as an initial value problem in time subject to boundary conditions. To obtain a well-posed problem, the boundary conditions may prescribe the normal components of **B** and **v**, and the tangential component of **E**. (In some cases the normal velocity may be related to the pressure and density through the characteristic equations. In the case of viscous flow the transverse component of the velocity must also be specified.) No other boundary conditions are required, or indeed may be specified.

We have developed several computer codes to solve Eqs. (1–7) in two and three spatial dimensions and time. These codes exactly preserve the solenoidal character of **B** and **J**, and need only the required number of boundary conditions.

Time integration of Eqs. (1–7) is difficult because of the widely separated time scales inherent in the model. These range from fast sound and Alfvén waves to slow resistive diffusion. Often the system is driven from the boundary (e.g., by shear motions) on some time scale that is slow compared to wave transit times but fast compared to global diffusion. In order to compute on these intermediate time scales, we have developed semi-implicit methods of time integration that allow these calculations to proceed economically. The accuracy and efficiency of these methods have been well documented (Schnack *et al.* 1990).

3. MODEL PROBLEMS OF CORONAL HEATING AND MAGNETIC RECONNECTION

Force-free Coronal Dynamics

The mechanism that heats the closed regions of the corona is unknown. Parker (1972) argued that the corona can be heated by resistive dissipation of electric current filaments that are induced by the long wavelength random twisting of the coronal magnetic field (see also van Ballegooijen 1985). The viability of this method of coronal heating requires that the current filaments attain a transverse scale length of $l \approx 10$ meters in response to photospheric flow of scale length $l_v \approx 10^4$ km. Theoretically, the question is twofold: can filamentary current structure form naturally from smooth, long wavelength photospheric motions; and, if these structures form, can their dissipation produce significant amounts of Ohmic heating?

Parker (1972) argued that discontinuities in the magnetic field will inevitably arise from a non equilibrium condition produced by the displacement of the field line footpoints. In a plasma with finite resistivity, these discontinuities are resolved into thin layers, called current sheets or filaments. Subsequently, numerical simulations of the response of a model three-dimensional coronal field to random footpoint motions have been performed. In one case, a sequence of ideal MHD equilibrium solutions was directly computed (van Ballegooijen 1988). In another case, the dynamical ideal MHD equations were solved to obtain a sequence of equilibria (Mikić, Schnack, & Van Hoven 1989). In both cases filamentary current structure was observed to build in the corona as a sequence of smooth, random photospheric flows was applied. The thinness of the filaments was limited only by the finite spatial resolution of the numerical calculations. There is no inherent limit to the thinness of these structures within the ideal MHD model. Thus, the first important theoretical question is answered in the affirmative.

We have begun to investigate the second theoretical question: namely, can these inevitable current filaments produce sufficient Ohmic power to significantly contribute to coronal heating? To this end, we have extended of our previous work to include the effects of finite electrical resistivity. Following Parker (1972), the corona is modeled in Cartesian (x,y,z) geometry, with $0 \le x \le L_x$, $0 \le (y,z) \le L$. The initial magnetic field is taken as a uniform field $\mathbf{B}_0 = B_0\hat{\mathbf{e}}_x$

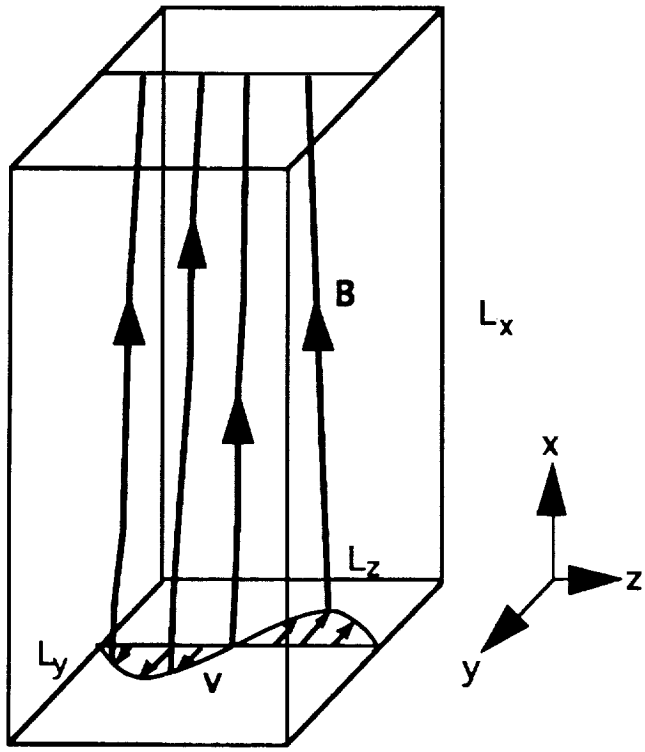

Figure 1. Geometry of model problem for coronal heating.

extending between two conducting plates. In this idealized configuration, these plates represent the photosphere to which both ends of the field lines are attached. Equilibrium field line curvature effects are thus not included in this model. The system is periodic in the transverse y and z directions; thus, the net longitudinal (x) current is constrained to be zero. Tangential photospheric flow is specified on one plate ($x = 0$), and the response the coronal field to these motions is given by the solutions of the MHD equations. The model is sketched in Fig. 1.

In the quiet corona, the magnetic energy density greatly exceeds the internal energy density of the coronal plasma, i.e., $\beta = 8\pi p/B^2 << 1$ (Tucker 1973). Since pressure forces are thus negligible, coronal equilibria are characterized by the vanishing of the Lorentz force, $\mathbf{J} \times \mathbf{B} = 0$. Magnetic field configurations that satisfy this condition are called force-free. In that case it proves convenient to ignore the pressure force in the dynamical equation of motion as well (Ortolani & Schnack 1993). In this approximation, the equation of state becomes $\nabla p = 0$. When the resistivity is finite, the dynamical Eqs. (1–7) are, in a convenient nondimensional form,

$$\frac{\partial \mathbf{B}}{\partial t} = \nabla \times (\mathbf{v} \times \mathbf{B}) + S^{-1} \nabla^2 \mathbf{B} \tag{8}$$

$$\rho_0 \frac{\partial \mathbf{v}}{\partial t} = -\rho_0 \mathbf{v}\cdot\nabla\mathbf{v} + \mathbf{J}\times\mathbf{B} + \nu\rho_0\nabla^2\mathbf{v} \qquad (9)$$

where ν is a viscosity and $S = \tau_R/\tau_A$ is the Lundquist number. The resistive diffusion time is $\tau_R = 4\pi L^2/c^2\eta$, η is the uniform, constant resistivity, L is a scale length transverse to the initial field, and the Alfvén transit time is $\tau_A = L/v_A$, where $v_A = B_0^2/(4\pi\rho_0)^{1/2}$ is the Alfvén velocity. Thus $S \rightarrow \infty$ is the limit of zero resistivity, or infinite conductivity.

Typical parameters for the quiet corona are (Parker 1983) $L_x \approx 10^{10}$ cm, $L_x/L \approx 4$, $B_0 \approx 10$G, $v_A \approx 7\times10^7$ cm/sec, $\tau_A \approx 14$ sec, $\eta \approx 4.8\times10^{-17}$ sec, and $\tau_R \approx 3\times10^{14}$ sec, which yields a value for the Lundquist number of $S \approx 2\times10^{13}$. This value of S is too large for finite numerical computation, as the number of degrees of freedom of the turbulent system will greatly exceed the storage capacity of present computers. Our strategy is to produce a series of calculations at lower, but yet still substantial, values of S , and examine the scaling of the results with S.

Beginning with this initial state, we introduce finite S and apply a sequence of thirty successive long wavelength photospheric flows. No attempt is made to relax to equilibrium between each successive flow application. The viscosity in Eq. (9) is taken to be $\nu = 2\times10^{-4}$. The driving flow velocity is $V_0 = 0.0125v_A$, corresponding to about 7 km/sec. (This is somewhat faster than observed flows in order to save computer time.) The duration of each step in the flow T is chosen to be $T = 50\tau_A$.

In externally driven flows, one definition of the fluid Reynolds' number R is the ratio of the viscous diffusion time to the driving time scale (the so-called eddy turnover time). For the parameters described above, we have $R = 62.5$. In order to retain numerical resolution at this viscosity, the Lundquist number was chosen as $S = 2\times10^4$.

As a result of this flow pattern, the footpoints of the magnetic field lines execute a random walk in the photosphere. For the parameters used in these calculations, the mean field line displacement per step and the stochastic diffusion coefficient become $\langle\lambda\rangle = 4.96\times10^7$ cm, and $D_{st} = 1.95\times10^{12}$ cm^2/sec. This diffusion coefficient is a factor of 2 smaller than that deduced from random motion of the supergranule boundary junctions (Parker 1983).

In Fig. 2 we plot the average value of the Lorentz force $\mathbf{J}\times\mathbf{B}$ in the corona as a function of time in response to the drive. Since the equilibrium corona is approximately force-free, large values of the Lorentz force indicate periods of intense dynamical activity. Note that there are two large, transient deviations from near-equilibrium conditions. In Fig. 3 we show details of the flow pattern in the vicinity of one of the current sheets that occur in response to the drive. This flow pattern is consistent with magnetic reconnection.

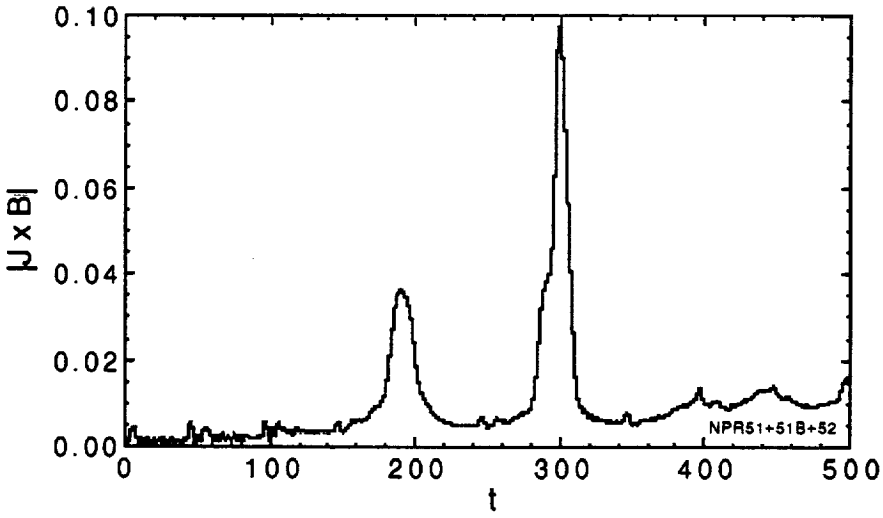

Figure 2. Average Lorentz force in the corona as a function of time.

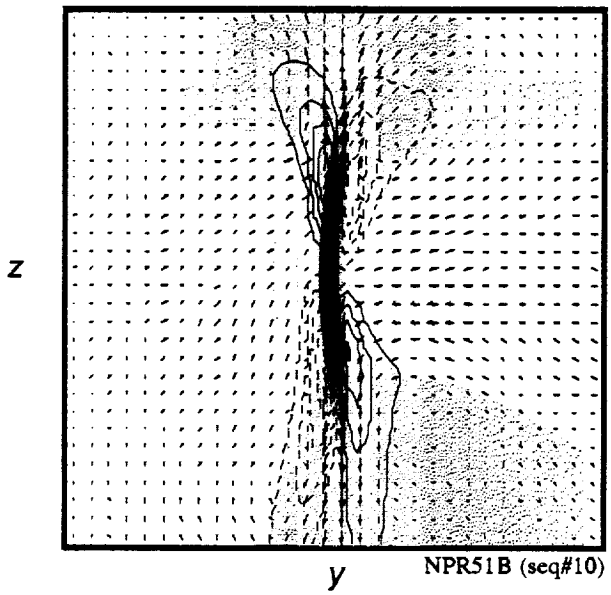

Figure 3. Transverse flow pattern in the vicinity of a current filament during dynamical phase.

These calculations have confirmed that: 1) fine scale current density filaments naturally and rapidly form in the corona in response to random, long wavelength footpoint displacements; 2) the Ohmic heating rate in this configuration is enhanced over what would arise from more broadly distributed currents; 3) transient magnetic reconnection occurs in these intense current filaments. These results have been described by Schnack & Mikić (1994). A more detailed manuscript is in preparation.

Magnetic Field Response to Simple Braiding Flows

The results presented above suggest that the tangling of field lines may lead inevitably to the formation of thin current structures. However, the random, statistical nature of the driving flow makes the results difficult to analyze. We thus seek a similar problem that is both relatively simple to analyze, and yet contains the essential ingredients of the phenomena.

It has been suggested (Vainshtein 1994) that braiding of magnetic field lines will result in the formation of current sheets. The argument is essentially as follows: Consider three braided field lines that stretch between two plates. As is necessary in a braid, the algebraic sign of the twist of any braided field line must change as the field line is traversed along its length from one plate to the other. This twist is related to the torsion of the field: $\alpha = \mathbf{J} \cdot \mathbf{B} / B^2$. But in a force free field α must be constant along a field line. Thus smooth force-free equilibrium is incompatible with braided fields, and the configuration must inevitably develop tangential discontinuities, or current sheets. (This has been called *magnetic non-equilibrium.*)

A simple photospheric flow that can produce braiding in the configuration shown in Fig. 1 is given by (Vainshtein 1994)

$$\psi = \psi_1 (y,z) \cos^2 \omega t + \psi_2 (y,z) \sin^2 \omega t \tag{10}$$

$$\mathbf{v} = \nabla \psi \times \hat{\mathbf{x}} \tag{11}$$

This flow produces alternating, overlapping Gaussians that twist the field lines about each other in a braiding manner.

In response to this driving flow, the current shows a filamentary structure. In Fig. 4 we plot the field lines on either side of a current filament after the introduction of resistivity ($S = 2 \times 10^4$). The change of topology that occurs is evident, and is characteristic of magnetic reconnection. The behavior is similar to that observed in the more complex case of random, long wavelength driving flows.

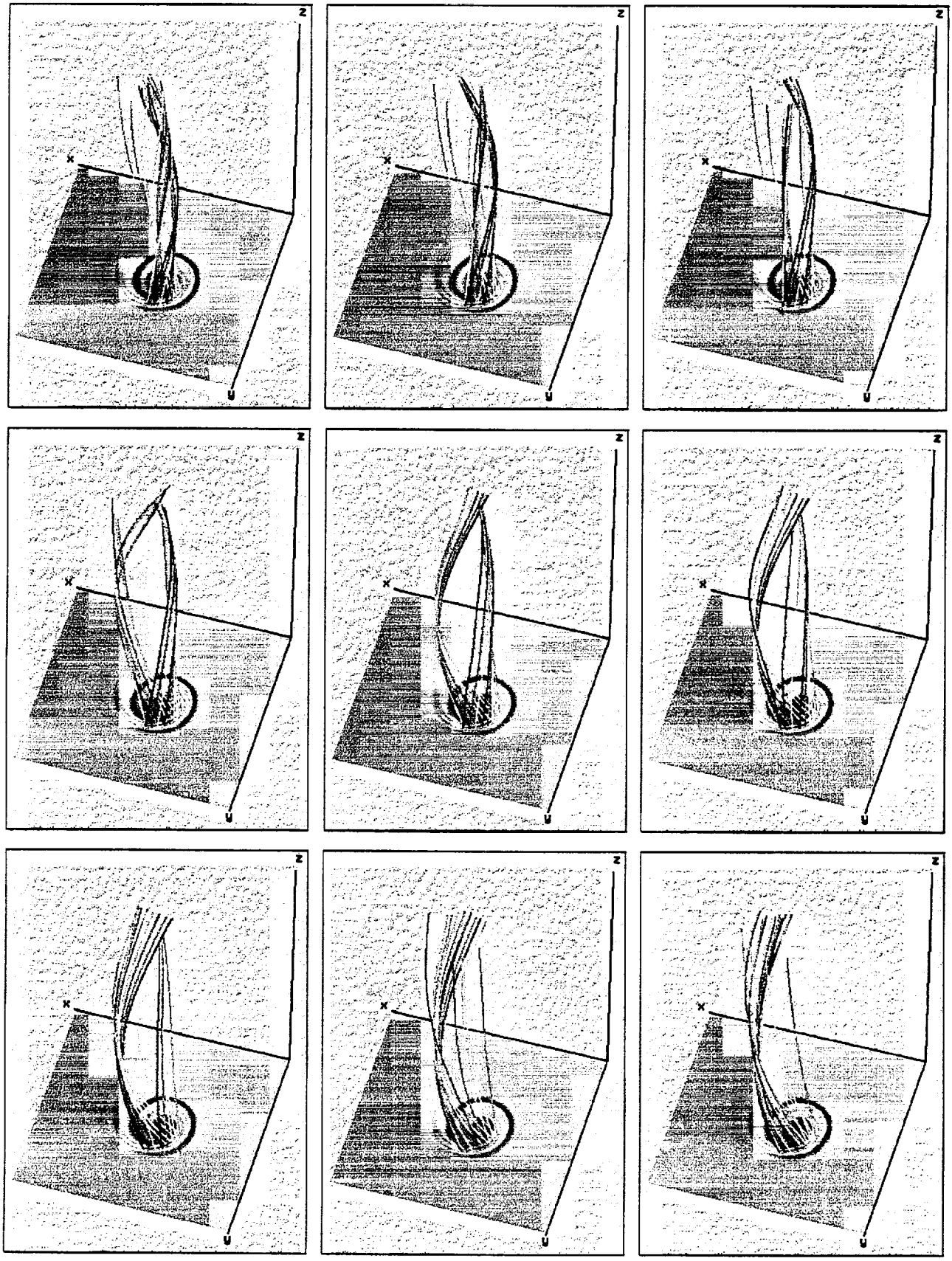

Figure 4. Evolution of magnetic field lines on either side of the current filament formed in response to braiding flow.

It appears that the essential dynamics that occur in the coronal heating problem can be reproduced with the simpler braiding flow described above. By further studying this problem, we hope to learn about the onset of magnetic nonequilibrium as a function of braiding. By performing the simpler calculation at different values of S we may be able to determine how this three-dimensional transient reconnection scales with resistivity.

Simple Model of Two-Dimensional, Spontaneous Reconnection

Conversion of magnetic energy into other forms (thermal and kinetic) is a primary aspect of solar activity. Magnetic reconnection is widely perceived to play an important role in this process; however, the question of how reconnection can proceed rapidly enough in the highly conducting solar plasma to account for the observed phenomena remains an open question. One candidate for fast, driven reconnection is the mechanism of topological dissipation (Parker 1972, 1979). By fast reconnection we mean that the rate of field annihilation should scale weakly or be independent of the Lundquist number S. Unless anomalous dissipation is present, reconnection rates that scale weakly with S are necessary to account for the rapid energy conversion observed in solar activity ($S \approx 10^{14}$ for the coronal plasma).

Parker (1972) established that motions at the footpoints of a uniform magnetic field can lead to sufficiently complex magnetic field topologies (such as braided flux tubes with several field lines wrapped around each other) that must exhibit tangential discontinuities in the field. The process in which an initially smooth magnetic field evolves into a configuration with discontinuities has been described as topological or magnetic nonequilibrium (Parker 1972, 1979; Priest 1981; Moffat 1985; Vainshtein & Parker 1986; Vainshtein, Bykov, & Toptygin 1993). Real plasmas have a finite resistivity, and the discontinuities are resolved into thin layers called current sheets. Parker (1979) argued that magnetic reconnection must proceed sufficiently rapidly at these sheets to dissipate the energy input by further footpoint motions.

Establishing or disproving that fast reconnection occurs in the three-dimensional systems previously described is a difficult computational task. Scaling the reconnection rate over a large range of S can be more easily accomplished in an idealized two-dimensional configuration. A two-dimensional configuration that is believed to exhibit magnetic nonequilibrium is the rosette configuration (Vainshtein, Bykov, & Toptygin 1993). Similar configurations have been studied in the context of the coalescence instability (Finn & Kaw 1977; Pritchett & Wu 1979; Richard *et al.* 1989; Longcope & Strauss 1993). In the starting configuration, two flux tubes with parallel current density are placed some distance apart. The configuration is not in equilibrium; the magnetic forces are such that the flux tubes will move towards each other. Vainshtein, Bykov, & Toptygin (1993) have argued that the resulting equilibrium

configuration in ideal MHD will exhibit a discontinuity, and that in resistive MHD, fast reconnection will occur.

We have first investigated the ideal (i.e., zero resistivity) behavior of attracting flux tubes. We note that simulating ideal MHD behavior when current sheets are present is not usually possible by standard numerical treatments of the MHD equations. In the absence of resistivity, the current sheet collapses to the mesh size and generates unphysical oscillations. However, we were able to develop a special treatment of the current sheet region that exploits the symmetry and allows the magnetic field to approach a discontinuous function (see Mikić & Linker 1994).

The initial and final configuration for the two flux tubes in the ideal MHD calculation is shown in Fig. 5. Contours of the flux function (projections of magnetic field lines) are shown on the left; a strong magnetic field out of the plane (approximately 10 times the field in the plane) is also present. The current density out of the plane is shown on the right. The first two frames show the initial state and the full simulation domain; the use of nonuniform meshes allows us to place the outer walls far away. The middle frames shows a close-up of the flux tubes in the initial state, and the bottom two frames show the final configuration, which the system relaxes to after about 100 Alfvén times (τ_A).

In the final state, the flux tubes have converged and a current sheet (of opposite sign to the current density in the flux tubes) forms between them. Our preliminary results (on a 151 × 151 nonuniformly spaced mesh) indicate that the current sheet thickness for this configuration is controlled by the mesh spacing and the configuration approaches a true discontinuity in ideal MHD. We plan to verify this on meshes as much as ten times more resolved than the present case.

We have also investigated the resistive evolution of this configuration. Figure 6 shows the evolution of the projected field lines when a finite plasma resistivity corresponding to $S = 10^4$ is included in the calculation (the flux tubes were also placed farther a part in the initial state). Times in Fig. 6 are given in τ_A (both τ_A and S are scaled by the total magnetic field). Figure 2 shows that the flux tubes merge together rapidly. We can estimate the reconnection rate for this case by computing $(dW/dt)/W$, where W is magnetic energy of the planar component of the field. Figure 7 shows this plotted over time (the rate is computed based on the planar Alfvén time); there is a sharp rise in the reconnection rate as the flux tubes approach each other. We plan to perform several calculations at different S to see how this rate scales with S. A wide range of S should be possible, because the two-dimensional nature of the problem allows one to place many mesh points in the vicinity of the current sheet.

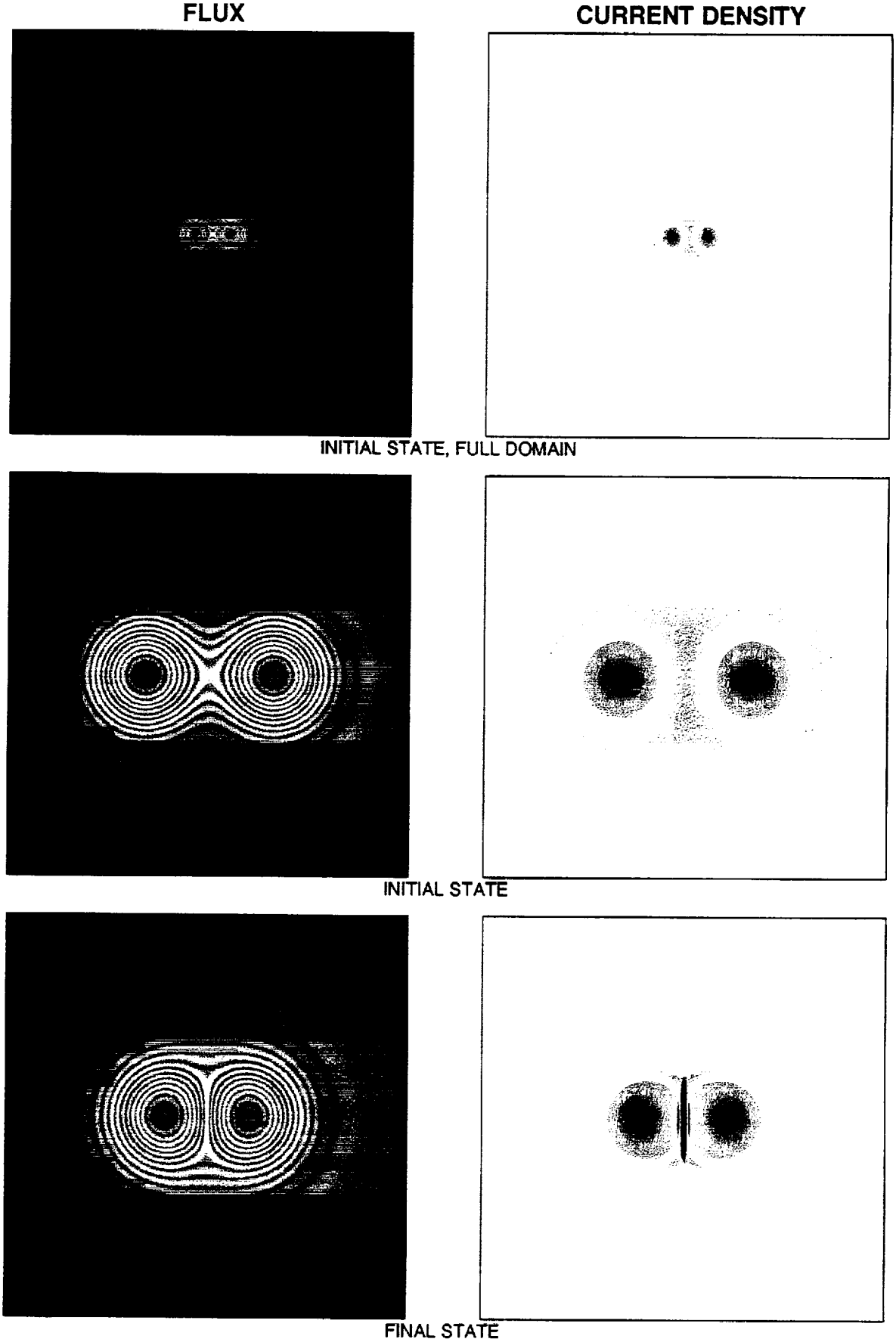

Figure 5. Initial and final configurations of merging flux tubes with zero resistivity (ideal MHD).

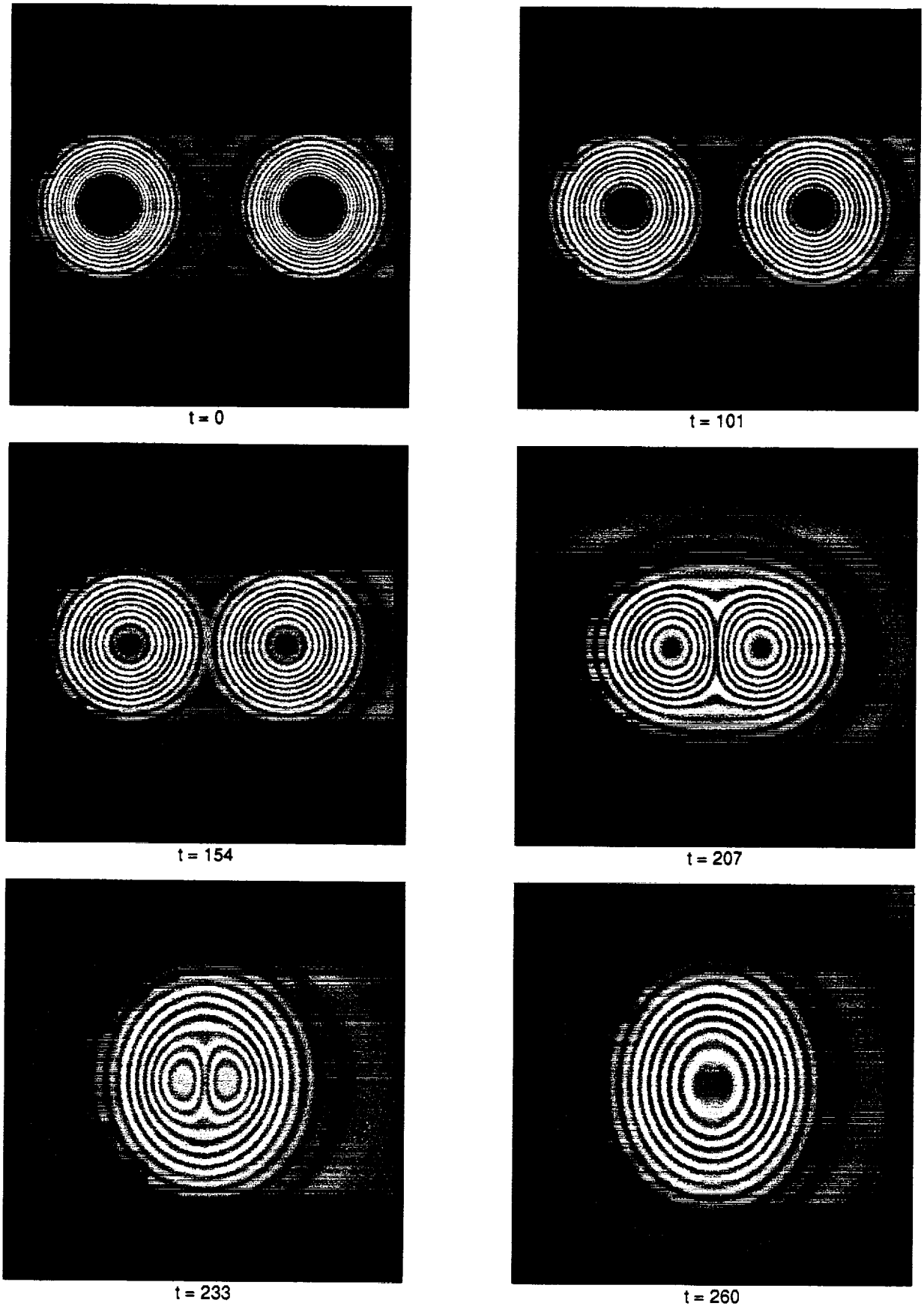

Figure 6. Evolution of merging flux tubes with finite resistivity ($S = 10^4$).

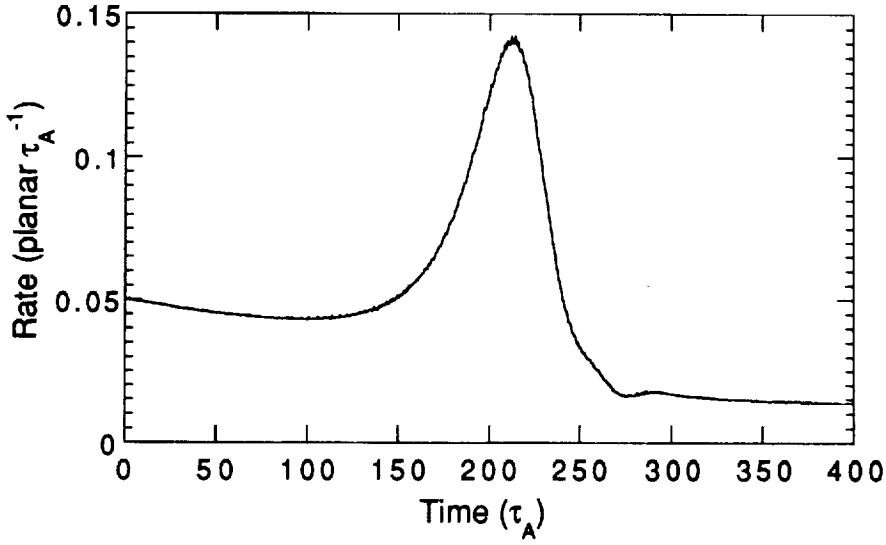

Figure 7. Reconnection rate vs. time for merging flux tubes with $S = 10^4$.

4. LARGE SCALE CORONAL DYNAMICS

In addition to the model problems discussed above, we have used the full set of resistive MHD Eqs. (1–7) to study large scale dynamics of the solar corona in spherical coordinates. In particular, we have been applying our models to the formation and disruption of helmet streamers, and the initiation and propagation of coronal mass ejections (CMEs). The calculations are global in the sense that they cover the entire sun and interplanetary space to distances beyond the earth's orbit (1 AU). Calculations of this magnitude are possible only because of the numerical methods described in Section 2.

Formation of a Helmet Streamer

Helmet streamer configurations have been modeled via numerical solution of the MHD equations by a number of authors (Pneumann & Kopp 1971; Endler 1971; Steinolfson, Suess, & Wu 1982; Washimi, Yoshino & Ogino 1987; Linker, Van Hoven, & Schnack 1990; Wang *et al.* 1992). One advantage of this approach is that it facilitates using the streamer model as the initial condition for other coronal simulations (Steinolfson & Hundhausen 1988; Linker, Van Hoven, & McComas 1992). We compute a two-dimensional (azimuthally symmetric) helmet streamer configuration by imposing a spherically symmetric transonic wind solution on an initially dipolar magnetic field and allowing the configuration to evolve in time until a steady state is reached. Spherically symmetric polytropic wind solutions were formulated by Parker (1963); these are

steady-state solutions of the 1-d mass and momentum equations for a gas that obeys the polytropic law p/ρ^{γ} = constant. Polytropic wind solutions have the advantage that relatively simple models can match many of the properties of the corona. However, values of γ close to 1 are necessary to produce radial density and temperature profiles that are similar to coronal observations; this reflects the fact that important thermodynamic processes, such as heating, radiation, and thermal conduction, have been omitted from the energy equation (Parker 1963). We choose γ = 1.05, as previous authors have done (Steinolfson, Suess, & Wu 1982; Washimi, Yoshino, & Ogino 1987).

With these initial and boundary conditions, Eqs. (1–7) were integrated forward in time for over 130 days (17,700 τ_A) to ensure that the configuration was in a steady state. Figure 8 shows the contours of the flux function $\psi = rA_{\phi}\sin\theta$ and contours of the azimuthal current density J_{ϕ}. Contours of ψ delineate magnetic field lines. The plasma is essentially stationary inside the closed-field region but flows outward along field lines in the open field region. The plasma density and pressure are larger in the closed-field region; the pressure force is balanced by the Lorentz force at the current sheets. The magnetic field is nearly potential everywhere except at the current sheets.

In Fig. 9 we show a reconstruction of the polarization brightness using integrated line-of-sight density from one of our calculations using a more complex flux distribution at the solar surface. This is how the calculated streamers might be viewed with a coronameter.

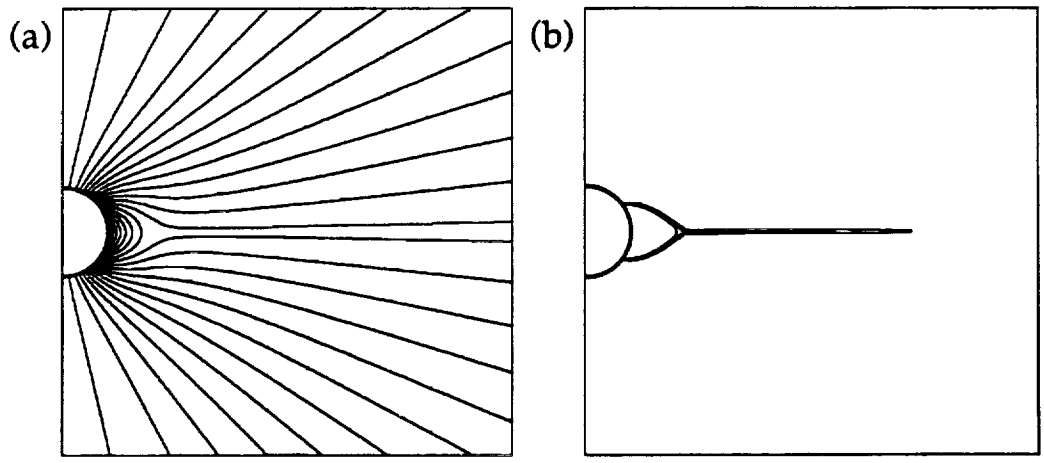

Figure 8. Contours of the flux function and azimuthal current density in a two-dimensional helmet streamer configuration.

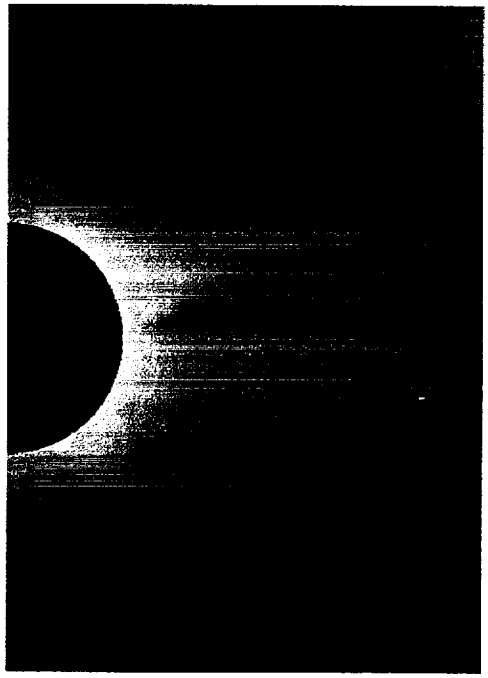

Figure 9. Reconstructed polarization brightness based on integrated line-of-sight density obtained from a calculated helmet streamer configuration.

Disruption of a Helmet Streamer

To investigate the effects of magnetic shear on a helmet streamer, we introduced a shearing motion at the photosphere and continued our time integration of the MHD equations. Figure 10 shows the evolution of ψ for the helmet streamer after shearing flows are introduced. Only a portion of the simulation domain is shown; the outer boundary is at 20 R_s. The ψ contours show projections of the magnetic field lines; the field also has a longitudinal component out of the plane. In response to the shear applied at the magnetic field footpoints, the closed-field region expands slowly, and the lower field lines beneath the helmet are squeezed towards the equator, causing J_ϕ to increase. Eventually the magnetic field lines erupt outward, the magnetic field reconnects, and a plasmoid is ejected into the outer corona.

Reconnection causes the nearly fully opened helmet streamer to reform. As the reconnection proceeds, the closed-field region grows in size as successively higher loops reconnect, a phenomenon that has been observed in recent Yohkoh soft X-ray images (Hiei, Hundhausen, & Sime 1993). After the helmet streamer reforms, it has a smaller closed-field region and higher magnetic energy than the initial streamer. With continued shearing, the streamer builds up more energy and disrupts again at approximately the same level of magnetic energy as the first disruption. The subsequent disruption events are very similar in character to the first event. The solar wind appears to contribute to the disconnection of the

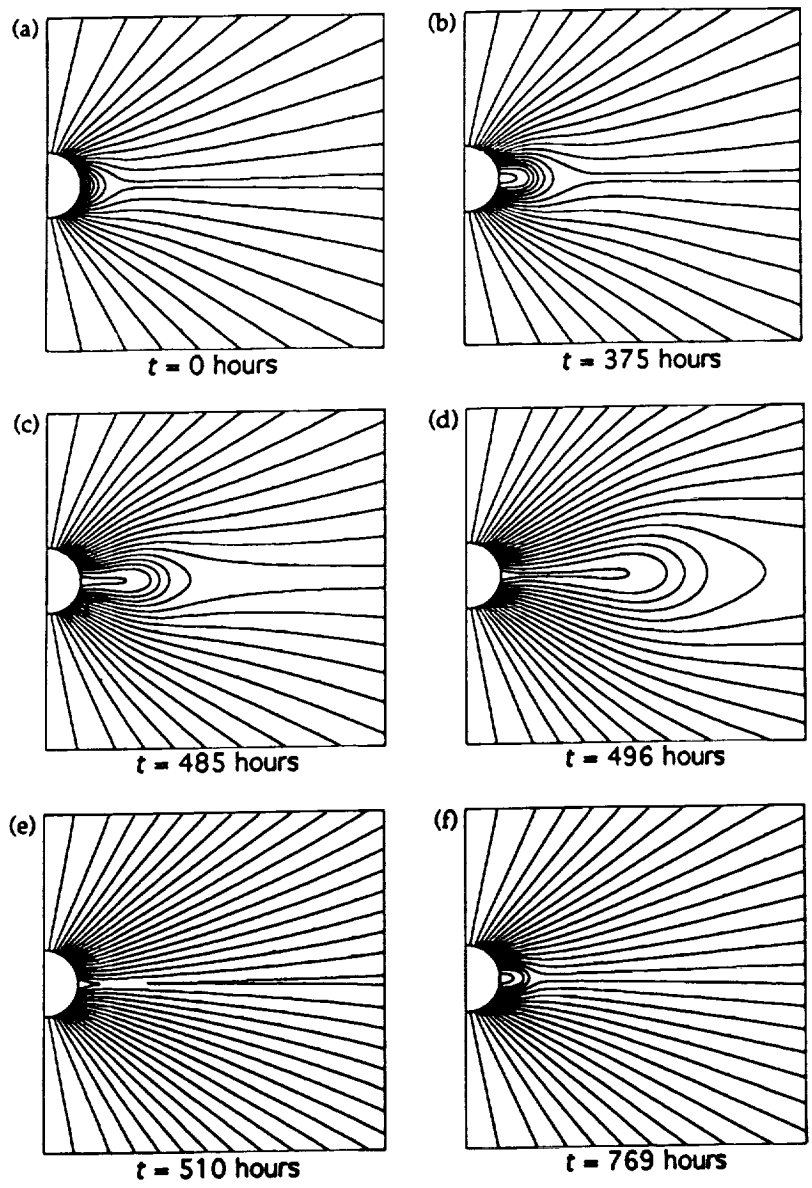

Figure 10. Evolution of the flux function for the helmet streamer in response to photospheric shearing flows.

plasmoid. Once the magnetic field expands upward, plasma on the field lines is accelerated by the local solar wind flow, dragging the magnetic field upward further until the field lines reconnect.

In the field of view of a coronagraph (e.g., 6 R_S for the Solar Maximum mission, MacQueen *et al.* 1980), the visible manifestations of the disruption described here would be associated with the initial upward movement of the magnetic field lines, which occurs well before the onset of magnetic reconnection. During this phase of the evolution, field lines that were originally very close to the coronal base rise to large heights in the corona. For example,

the field line with a height of 1.03 R_s at its apex in the unsheared helmet streamer rises to a height of 4.8 R_s before disconnecting from the photosphere. Therefore, if a low-lying prominence were embedded in this helmet streamer, it would erupt outward, as is often observed in CMEs. These results are described by Linker & Mikić (1994). The physics underlying the disruption is described by Mikić & Linker (1994).

Propagation of a CME to 1 AU

One paradigm for the cause of terrestrial magnetic storms is the passage of a CME launched from the sun past the earth's orbit (1 AU ~ 215 R_s) (Gosling 1993; Hundhausen 1994). As an initial test of this hypothesis, we have used our computational models to form and disrupt a helmet streamer and then follow the trajectory of the resulting plasmoid through interplanetary space past 1 AU, all in the same calculation. We can then determine the effect of the passage of the plasmoid on the interplanetary magnetic field (IMF) at earth, and see if it is consistent with signatures of the onset of magnetic storms. These are the first steps in a self-consistent model of "space weather."

In order to determine the effect of the passage of a CME on the IMF at earth, the spiral form of the solar field due to the sun's rotation must be reproduced. We do this by introducing solar rotation after the formation of the steady-state helmet streamer configuration described in the previous paragraphs. The rotation of the sun is then viscously and magnetically coupled to the solar wind, and its effect can propagate into the IMF as Alfvén waves. After approximately 3.8 solar rotations (~ 100 earth days) a new steady-state configuration is reached. The spiral structure of the IMF is shown in Fig. 11.

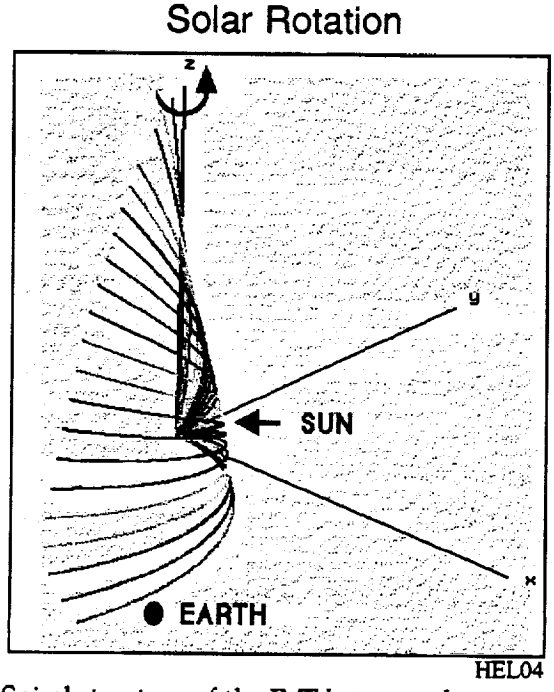

Figure 11. Spiral structure of the IMF between the sun and the earth.

In Fig. 12 we show detail of this configuration near the sun. Note the closed helmet structure that remains.

This structure is then subjected to photospheric shear, as described previously. The resulting disruption appears much as in the case with no rotation, except we now continue the calculation until the disturbance passes 1 AU. The perturbation in the IMF at earth during the passage is shown in Fig. 13. (Here, B_θ is the "north-south" component as viewed from earth.) The passage clearly induces a southward (negative B_θ) component of the IMF. Southward IMF has been correlated with the onset of terrestrial magnetic storms.

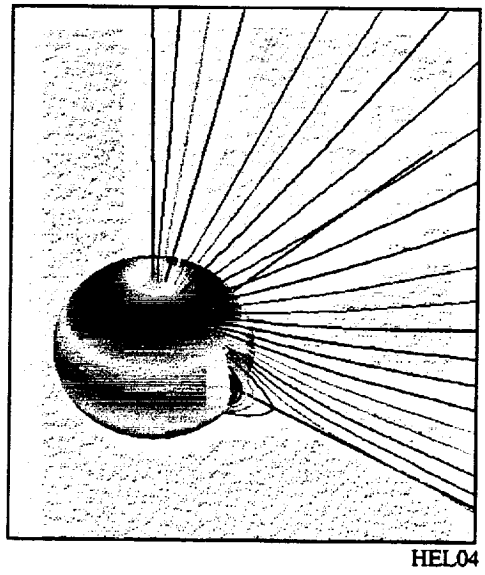

Figure 12. Detail of magnetic field near the sun for the configuration shown in Figure 11. The helmet streamer is visible.

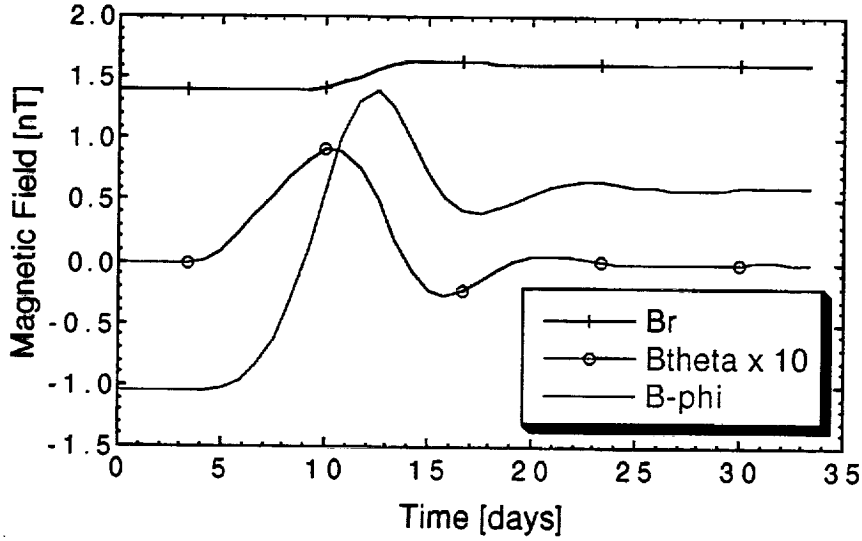

Figure 13. Computed perturbation to the IMF at earth during the passage of a CME.

REFERENCES

Endler, F. 1971, Ph.D. Thesis, Gottingen Univ.

Finn, J. M., & Kaw, P. K. 1977 *Phys. Fluids*, **20**, 72.

Gosling, J. T. 1993, *J. Geophys. Res.*, **98**, 18937.

Hiei, E., Hundhausen, A. J., & Sime, D. G. 1993, *Geophys. Res. Lett.*, **20**, 2785.

Hundhausen, A. J. 1994, *EOS,Trans. AGU* **75**, 312.

Linker, J. A., Van Hoven, G., & Schnack, D. D. 1990, *Geophys. Res. Lett.* **17**, 2281.

Linker, J. A., Van Hoven, G., & McComas, D. J. 1992, *J. Geophys. Res.*, **97**, 13733.

Linker, J. A., & Mikić, Z. 1994, *Astrophys. J.*, submitted.

Longcope D. W., & Strauss, H. R., 1993 *Phys. Fluids* **B5**, 2858.

Lu, E. T., & Hamilton, R. J. 1991 *Astrophys. J.* **380**, L89.

MacQueen, R. M., Csoeke-Poeckh, A., Hildner, E., House, L., Reynolds, R., Stanger, A., Tepoel, H., & Wagner, W. 1980, *Sol. Phys.*, **65**, 91.

Mikić, Z., Schnack, D. D., and Van Hoven, G. 1989 *Astrophys. J.*, **338**, 1148.

Mikić, Z., & Linker, J. A. 1994, *Astrophys. J.*, in press.

Moffat, H. K. 1985, *J. Fluid Mech.*, **159** 359.

Ortolani, S., & Schnack, D. D. 1993, *Magnetohydrodynamics of Plasma Relaxation*, World Scientific, Singapore.

Parker, E. N. 1963, *Interplanetary Dynamical Processes*, Interscience publishers, New York.

Parker, E. N. 1972, *Astrophys. J.* **174**, 499.

Parker E. N. 1979, *Cosmical Magnetic Fields* , Clarendon Press, Oxford.

Parker, E. N. 1983, *Astrophys. J.*, **264**, 642.

Pneuman, G. W., & Kopp, R. A. 1971, *Sol. Phys.*, **18**, 258.

Priest, E.R. 1981, in *Solar Flare Magnetohydrodyanmics*, ed. E. R. Priest, Gordon and Breach, London, pp. 142 and 150.

Pritchett, P. L., & Wu, C. C. 1979, *Phys. Fluids*, **22**, 2140.

Richard, R. L., Walker, R. J., Sydora, R. D., & Ashour-Abdalla, M. 1989, *J. Geophys. Res.*, **94**, 2471.

Schnack, D. D., Mikić, Z., Barnes, D. C., & Van Hoven, G. 1990, *Comput. Phys. Comm.*, **59**, 21.

Schnack, D. D., & Mikić, Z. 1994, *Proc. 1993 Sacramento Peak Workshop on Coronal Dynamics*, Sunspot, NM.

Steinolfson, R. S., Suess, S. T., & Wu, S. T. 1982, *Astrophys. J.*, **255**, 730.

Steinolfson, R. S., & Hundhausen, A. J. 1988, *J. Geophys. Res.*, **93**, 14269.

Vainshtein, S. I., & Parker, E. N. 1986, *Ap. J.*, **304**, 821.

Vainshtein, S. I., Bykov, A. M., and Toptygin, I. N., 1993, *Turbulence, Current Sheets and Shocks in Cosmic Plasma* , Gordon and Breach, Amsterdam.

Vainshtein, S. 1994 , private communication.

van Ballegooijen, A. A. 1985, *Astrophys. J.*, **298**, 421.

van Ballegooijen, A. A. 1988, *Proc. Ninth Sacramento Peak Summer Workshop on Solar and Stellar Coronal Structure and Dynamics*, ed. E. Altrock, Sunspot, New Mexico, p115.

Tucker, Wallace H. 1973, *Astrophys. J.***186**, 285.

Wang, A. H., Wu, S. T., Suess, S. T., & Poletto, G. 1993, *Sol. Phys.*, **147**, 55.

Washimi, H., Yoshino, Y., & Ogino, T. 1987, *Geophys. Res. Lett.*, **14**, 487.